

Elaboration of Materials with Functionality Gradients by Assembly of Chitosan-Collagen Microspheres Produced by Microfluidics

David Azria^{1,2}, Raluca Guermache^{1,2}, Sophie Raisin¹, Sébastien Blanquer¹, Frédéric Gobeaux³, Marie Morille¹ and Emmanuel Belamie^{1,2,*}

¹ICGM-MACS, UMR 5253 CNRS-ENSCM-UM, Charles Gerhardt Institute Montpellier, 8 rue de l'Ecole normale, 34296 Montpellier cedex 5, France

²Ecole Pratique des Hautes Etudes, PSL Research University, 75014 Paris, France

³LIONS—NIMBE CEA, CNRS, University of Paris-Saclay, CEA Saclay, 91191 Gif-sur-Yvette, France

Received May 31, 2017; Accepted November 24, 2017

ABSTRACT: Biopolymers extracted from renewable resources like chitosan and collagen exhibit interesting properties for the elaboration of materials designed for tissue engineering applications, among which are their hydrophilicity, biocompatibility and biodegradability. In many cases, functional recovery of an injured tissue or organ requires oriented cell outgrowth, which is particularly critical for nerve regeneration. Therefore, there is a growing interest for the elaboration of materials exhibiting functionalization gradients able to guide cells. Here, we explore an original way of elaborating such gradients by assembling particles from a library of functionalized microspheres. We propose a simple process to prepare chitosan-collagen hybrid microspheres by micro- and milli-fluidics, with adaptable dimensions and narrow size distributions. The adhesion and survival rate of PC12 cells on hybrid microspheres were compared to those on pure chitosan ones. Finally, functionalized microspheres were assembled into membranes exhibiting a functionalization gradient.

KEYWORDS: Hybrid microspheres, biomaterials, chitosan, collagen, functionality gradient, nerve regeneration, microfluidics

1 INTRODUCTION

Materials can be elaborated with physical (topology, dimensionality, rigidity), chemical and biochemical cues designed to orient the behavior of cells [1–4]. More specifically, the control of neural differentiation and the guidance of neurite outgrowth is a very active research field [5–10]. It has been shown in many previous works that immobilized gradients of growth factors can induce the differentiation of neural cells and orient the neuritic outgrowth along the growth factor gradient [6, 7, 11, 12]. The generation of growth factor gradients has been achieved by several approaches, including microfabrication [13], the surface modification of polymers [6] or microfluidic technologies [14], providing a whole range of materials well adapted for *in-vitro* cellular studies. Fewer, however, are truly suited for *in-vivo* use as implantable material to promote and

guide nerve tissue regeneration. Hydrogels composed of biopolymers like chitosan and collagen have the advantage of being hydrophilic, biocompatible and biodegradable. Chitosan is a derivative of chitin, a very abundant polysaccharide generated as an industrial waste in large fisheries. As an example, the annual production of crustacean shell processing wastes by the Indian seafood industry amounts to about 100,000 tons/year [15]. Chitosan, as well as its chemical derivatives [16], have long been demonstrated to be highly relevant candidates for biomedical applications [17]. Apart from showing excellent biocompatibility and being bioresorbable, chitosan also exhibits one main functional group (amine $-NH_2$) highly suited for site-specific modification using EDC-based coupling techniques. Because the pKa of the amine group is roughly comprised between 6 and 7.5 depending on its degree of acetylation [18], chitosan is readily soluble at acidic pH and precipitates at neutral and basic pH. Collagen is a protein present in major extracellular matrices (ECM) like skin, bone or tendon, in the form of fibrils. Most cells express specific collagen

*Corresponding author: emmanuel.belamie@enscm.fr

DOI: 10.7569/JRM.2017.634186

receptors, called integrins, which are located at the cell membrane. Noncovalent interactions of the extracellular part of integrins with collagen fibrils provide anchoring points to the cells within the matrix, thus promoting cell adhesion. Collagen is often extracted from rat tail tendon for academic research purposes, but it is also available as an industrial product from bovine and porcine sources. Collagen is a triple helical protein which can be dissolved in acidic aqueous solutions and precipitate in the form of striated fibrils over a wide pH range around neutrality (6–12) [19]. This pH-induced precipitation of fibrils is associated with the formation of elastic gels, provided the collagen concentration is high enough, ca. ~ 10 mg/ml. Like chitosan, it is largely used for biomedical applications [20, 21], among which is nerve regeneration [21, 22].

In the present work, our intent was to generate microspheres as a cell-supporting material through a microfluidic-based process. Collagen was successfully used in a microfluidic device at a concentration of 3.5 mg/ml to encapsulate cells [23]. However, collagen solutions at a concentration high enough to produce strong gels suitable for material assembly (~ 10 mg/ml) are strongly viscoelastic [24] and difficult to handle in microfluidic devices. An alternative would be to use solutions at a much lower concentration, hence less viscous, and to covalently crosslink the particles with chemical agents like glutaraldehyde. To avoid the use of potentially toxic chemicals for the formation of stable microspheres, we studied the possibility to process chitosan solutions into microspheres by microfluidics and incorporate small amounts of collagen. This hybrid composition is attractive because it combines the relatively low viscosity of chitosan solutions with the property of collagen to promote cell adhesion. Such a combination has already proven suitable to support cell adhesion and tissue regeneration [25, 26].

Hydrogels formulated as microparticles offer the advantages of high surface area and injectability. The assembly of microparticles also provides an opportunity to generate materials with multiple functionalities without the necessity of site-specific post-modifications. This approach can be an interesting alternative to microprocessing techniques, like bio-printing, when the sensibility of biopolymers to processing conditions (high temperature, electric fields, light irradiation...) can be an issue. Milli- and microfluidic devices can be used to generate emulsions with controlled and homogenous dimensions. The characteristics and properties of the resulting materials are influenced by both intrinsic properties of the polymers, like their viscosity and ability to form gels, as well as processing parameters like the chip geometry and flow rates [27].

Here we studied the formation of chitosan microspheres by solidification of an acidic emulsion by raising the pH. In this process, we used no covalent crosslinking agent to stabilize the microspheres. Collagen was added to the initial chitosan acidic solution to elaborate hybrid particles and enhance cell adhesion by providing biochemical cues reminiscent of the extracellular matrix. We investigated the effect of mixing the two biopolymers on the processing conditions and resulting microspheres' morphology, dimensions and the biopolymers repartition. Cell adhesion was qualitatively assessed for both kinds of microspheres with PC12 cells. Finally, microspheres were modified and assembled to elaborate materials exhibiting a functionalization gradient. The proof of concept was demonstrated with a fluorescent dye covalently attached to the microspheres and then extended to a model protein.

2 EXPERIMENTAL

2.1 Biopolymers

- Chitosan powder (France Chitin, batch # 342) was solubilized in 0.1 M HCl, and the resulting solution successively filtrated on 8 μm , 0.8 μm , 0.45 μm and 0.22 μm membranes to remove insolubles. To regenerate the free amine form, chitosan was then precipitated by adding 10 M NaOH under stirring (1500 rpm) until pH 10 and the precipitate was retrieved by centrifugation at $3900 \times g$ for 20 min. The pellets were rinsed twice with a large volume of Milli-Q water, frozen at -80°C for 48 h, and finally freeze-dried. Sample solutions were prepared from ground chitosan powder solubilized in 0.5 M acetic acid. A molecular weight of 260 kDa was determined by SEC-MALLS (size exclusion chromatography coupled with multi-angle laser light scattering) using an UHPLC Thermo Scientific Dionex UltiMate 3000 with a Shimadzu RID-20A RI Detector and Wyatt miniDAWN TREOS MALLS instrument, GE Healthcare Superdex 200 10/300 GL column and an acetate buffer as the mobile phase (acetic acid 0.2 M, ammonium acetate 0.15 M, pH 4.5, 0.02 % NaN_3). Intrinsic viscosity of 11.1 dl/g was calculated by measuring dynamic viscosity at increasing concentrations (from 0.1 to 0.7 g/dl) with an Anton Paar rheometer in the cone-plate geometry (mobile CP50-1: diameter of 49.966 mm, cone angle 0.990° , cone truncation 99 μm). The deacetylation degree was determined at around 80 % by ^1H NMR according to the method presented in [28].

- Type I collagen was extracted and purified from young rat tail tendons following a protocol previously published [19]. Briefly, tendons were excised from the tail by dislocating the vertebrae, extensively rinsed in sterile phosphate-buffered saline (PBS) buffer to remove cells and traces of blood. Remaining cells were lysed by soaking the extracted tendons in NaCl 4 M followed by extensive washing with PBS before solubilization of the collagen in 0.5 M acetic acid. The resulting solution was clarified by centrifugation ($21,000 \times g$ for 2 h) to eliminate aggregates and collagen further purified from other proteins by selective precipitation. An acidic solution was finally prepared at 9 mg/ml in 0.5 M acetic acid by reverse osmosis against 50 g/l PEG 20 kDa. Collagen concentration was determined from the acidic solution before fibrillogenesis by assessing the amount of hydroxyproline [29].
 - Hybrid solutions were prepared with a chitosan:collagen mass ratio of 9:1. Chitosan and collagen solutions were prepared in acetic acid 0.5 M, mixed under magnetic stirring (250 rpm, at least 24 hours) to obtain a solution with a total polymer concentration (chitosan + collagen) of 2.1 % w/v (pH 3.88). To assess the homogeneity of the final solution, chitosan was labeled with fluorescein isothiocyanate (FITC) fluorochrome (1 FITC/2000 chitosan amine groups), and collagen with tetramethylrhodamine isothiocyanate (TRITC) (1 FITC/5000 collagen amine groups). The resulting microspheres were imaged by confocal microscopy (Leica Confocal SPE) at a 1024×1024 pixels resolution with 41 slices in the Z-dimension (Z stack), corresponding to a voxel size of $179.2 \times 179.2 \times 4657.7$ nm. 3D image reconstruction was done with ImageJ.
- of the junction were either $50 \times 50 \mu\text{m}^2$ or $100 \times 100 \mu\text{m}^2$ (respectively referred to as T50 and T100). Channel height was 76–80 μm , as determined by interferometry.
- T-junction: PEEK MicroTee (1/16 in) device (Upchurch) with a thru hole of 150 μm and corresponding tubing (1/16 in) were alternatively used to generate the emulsion. Before use, the inner surfaces of all fluidic parts were washed with pure acetic acid, dried at 80 °C overnight, coated with Sigmacote (Sigma, France) cured for 40 min at 80 °C to prevent wetting by the polymer solution.
 - Microspheres were produced with either a microfluidic chip or MicroTee device. Perfluorinated oil (3M™ Novac™ 7500 Engineered Fluid) was used as the oil phase with 1 wt% of a triblock copolymer surfactant synthesized in the lab according to a previously published protocol [30]. Unless otherwise stated, the flow rates were 0.02 ml/min for the oil phase and 0.002 ml/min for the aqueous phase. Both solutions were pumped into the milli-/micro-fluidic devices with a push syringe (Harvard Apparatus). Emulsion droplets were collected in a plastic Petri dish, covered with a layer of silicone oil. The Petri dish was then placed in an ammonia atmosphere to increase the pH and induce the precipitation of chitosan and the fibrillation of collagen. The solidified microspheres were then separated from the oil by cycles of centrifugation and washing with PBS.
 - The dimensions and size distributions of emulsion droplets and microspheres were determined by measurements performed on microscope images obtained with a Leica inverted microscope equipped with a CCD camera. Mean diameter and standard deviation were calculated from at least 100 measurements for droplets and 50 for microspheres.
 - Functionalization procedures: To visualize the formation of functionalization gradients, hybrid microspheres were labeled directly with a fluorescent probe (FITC) or with a model protein bovine serum albumin (BSA) itself modified with FITC (Sigma-Aldrich, A9771). Briefly, FITC was first dissolved in ethanol at 10 mg/ml, then diluted at 0.1 mg/ml in morpholinoethanesulfonic acid (MES 10 mM, pH 6). The required amount of FITC (from 1 FITC/2000 chitosan amine groups to 1/40000) was mixed with 50,000 microspheres suspended in PBS (final ratio MES:PBS of 25:75) under rotative agitation (10 rpm) overnight,

2.2 Milli- and Micro-Fluidics

- Microfluidic chips were prepared with Silicone (Sylgard 184 PDMS, Dow Corning) and 10 % hardening agent degassed by centrifugation (1000 rpm at ambient temperature), poured into a master mold and degassed again under vacuum for 10 min. The silicone was cured at 65 °C for 45 min, individual circuit chips were removed from the master mold before entrance and exit holes were punched. Individual chips were finally attached to a glass slide activated by plasma treatment (Dierner Plasma Femto 1). The emulsion was generated thanks to a flow-focusing geometry, and the lateral dimensions

protected from light. Microspheres were then rinsed 3 times with PBS to remove noncovalently bound fluorescein. Similarly, BSA-FITC was grafted onto microspheres. In MES 10 mM, succinic acid was activated with EDC (N-(3-Dimethylaminopropyl)-N'-ethylcarbodiimide hydrochloride) and reacted with microspheres suspended in PBS (final ratio of MES:PBS was 25:75) and molar ratio BSA-FITC:succinic acid:EDC was 1:10:80.

- Assembly of scaffold with function gradient: Microspheres were assembled by sedimentation and chemically crosslinked in a mold composed of two glass slides separated by a 0.8 mm thick U-shape spacer. Reticulation agents used were glutaraldehyde (at a 0.25 % final concentration) or succinic acid (60 mM) activated with EDC (240 mM). The mold containing microspheres and reticulation agent was centrifuged at 1600 g for 5 min at ambient temperature. After one hour of reaction, the assembled membranes were unmolded and extensively rinsed with PBS.

2.3 Cell Culture and Observations

- PC12 cells were cultured in DMEM completed with 10 % horse serum, 5 % fetal bovine serum, 1 % glutamine and 1 % penicillin/streptomycin. PC12 cell adhesion onto microspheres was assessed in DMEM 1 % glutamine and 1 % penicillin/streptomycin in Ultra-Low Adhesion 24-wells plates. The medium was removed and cells/microspheres were fixed with 1 ml

paraformaldehyde 3.7 % for 20 min, washed three times with PBS and transferred into 1.5 ml tubes. Cells/microspheres were stained with DAPI (1 ml at 1 $\mu\text{g}/\text{ml}$, 5 min) and washed three times with PBS. Observations of cell culture and cell adhesion onto microspheres were assessed with a EVOS FL Cell Imaging System (Thermo Fisher Scientific).

3 RESULTS AND DISCUSSION

3.1 Elaboration of Microspheres by Microfluidics

The microspheres were obtained by the initial formation of an emulsion with the biopolymers in the aqueous phase at acidic pH followed by solidification of the droplets. Both chitosan and collagen are soluble in acidic aqueous media but insoluble at neutral pH. The simplest way of solidifying the droplets was thus to induce a pH increase, which can be obtained by placing the acidic emulsion in the presence of ammonia vapors. This process allowed for the preparation of pure chitosan microspheres (Figure 2b) and of hybrid chitosan-collagen microspheres (Figure 2d) without chemical crosslinking agent, provided the initial biopolymers concentration was high enough to produce solids (gels) upon precipitation [31].

With both chitosan and hybrid solutions, homogeneous emulsions were produced (Figure 2a,e) with similar droplet size (Table 1). After precipitation by exposition to ammonia vapors, solid microspheres

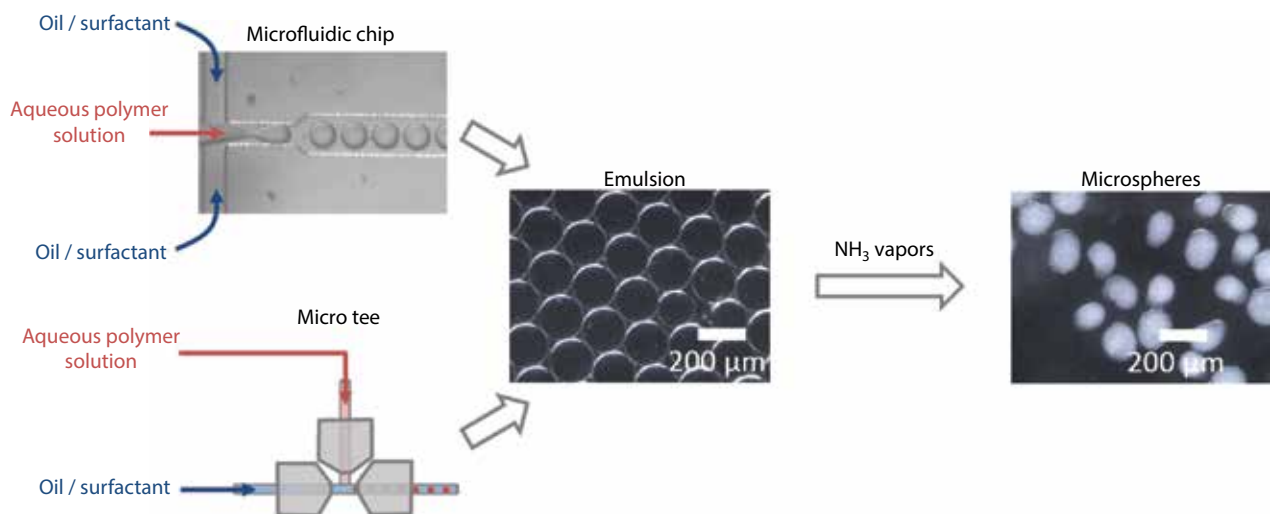


Figure 1 General scheme for formation of microspheres: The initial emulsion is obtained with an acidic polymer solution and oil/surfactant mixture, with either a microfluidic chip or a MicroTee device. Microspheres are then obtained by solidifying the emulsion under ammonia vapors.

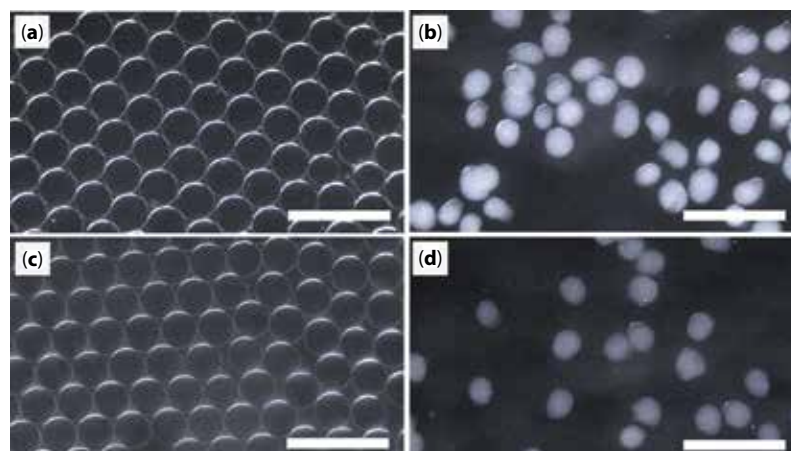


Figure 2 Images of emulsion droplets and microspheres generated with the T-junction millifluidic device: (a) chitosan emulsion, (b) chitosan microspheres after ammonia vapors, (c) chitosan-collagen hybrid emulsion, (d) hybrid microspheres after ammonia vapors. Micrographs (a–d) were taken under darkfield illumination. Scale bar: 500 μm .

Table 1 Emulsion droplet and microsphere size as a function of flow rates. Q_c/Q_d is the flow rate ratio between the oil (continuous phase Q_c) and chitosan or hybrid (chitosan:collagen, 9:1) aqueous phase (dispersed phase Q_d). The emulsion was obtained with either a microfluidic chip, $100 \times 100 \mu\text{m}^2$ (T 100) or $50 \times 50 \mu\text{m}^2$ (T 50) or a MicroTee device.

Chitosan	Flow rates ($\text{ml}\cdot\text{min}^{-1}$)			Diameter \pm SD (μm)		Size reduction / NH3 (%)
	Q_c	Q_d	Q_c/Q_d	Emulsion	μ -Spheres	
Chip T 50	0.05	0.002	25	60.67 ± 0.26	49.99 ± 5.88	18
	0.06	0.002	30	61.76 ± 3.01	52.29 ± 1.84	15
	0.07	0.002	35	57.55 ± 1.77	49 ± 1.37	15
Chip T 100	0.01	0.002	5	103.96 ± 3.83	81.08 ± 7.85	22
	0.02	0.002	10	95.24 ± 11.94	73.61 ± 11.48	23
	0.02	0.002	10	94.55 ± 10.81	68.61 ± 7.84	27
	0.02	0.003	6.67	101.44 ± 2.87	76 ± 7.09	25
	0.02	0.004	5	173.12 ± 5.32	140.62 ± 11.4	19
	0.03	0.002	15	81.96 ± 5.7	62.54 ± 6.49	24
	0.04	0.002	20	91.17 ± 9.74	68.46 ± 6.83	25
MicroTee	0.02	0.002	10	175.26 ± 10.2	135.03 ± 23.4	23
Hybrid						
Chip T 100	0.02	0.002	10	152.44 ± 2.99	124.74 ± 3.27	18
	0.04	0.002	20	130.22 ± 2.93	97.43 ± 26.96	25
	0.06	0.002	30	95.81 ± 10.69	67.41 ± 31.8	30
MicroTee	0.02	0.002	10	173.56 ± 4.9	136.24 ± 15.1	21

were formed and could be separated from the oil phase by filtration and successive rinsing steps.

As the pH-induced sol-gel transition proceeds, the droplets clearly shrink and slightly deform as the biopolymers precipitate forming hydrogel microparticles (Figure 2b,d). This shrinkage, reported in Table 1,

amounts to approximately 20–25 % of the initial droplet size for chitosan microspheres. It mostly results from the reduction of repulsive interactions as the pH goes beyond the pK_a of chitosan and solvent released, as largely described previously. Apparently, despite a slight deformation of the initial spherical morphology

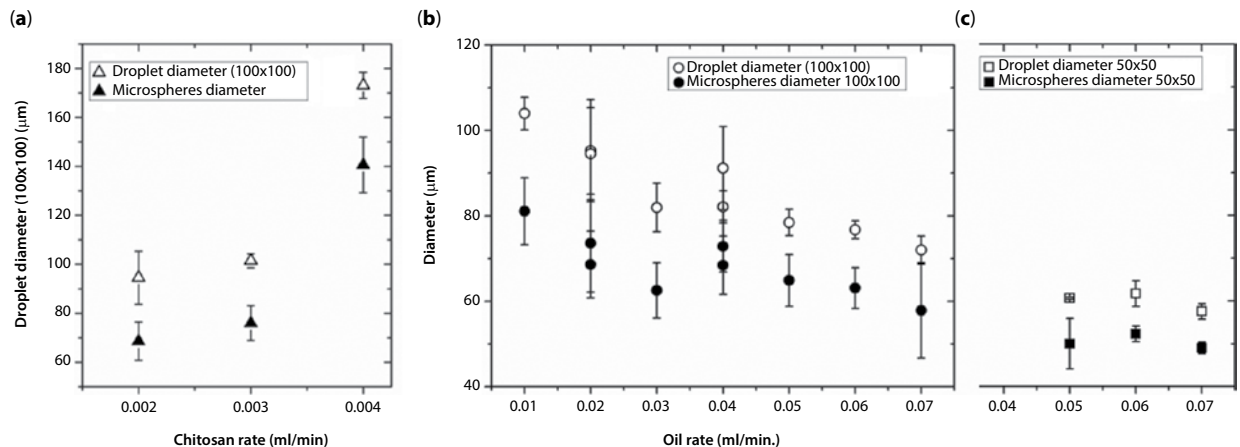


Figure 3 Size of emulsion droplets (open symbols) and microspheres after ammonia vapors (solid symbols): (a) as a function of chitosan solution flow rate at constant oil flow rate ($0.02 \text{ ml}\cdot\text{min}^{-1}$) and (b) as a function of oil flow rate at constant chitosan solution flow rate ($0.002 \text{ ml}\cdot\text{min}^{-1}$). The emulsion was obtained on a microfluidic chip with a $100 \times 100 \mu\text{m}^2$ (a, b) or $50 \times 50 \mu\text{m}^2$ (c) cross design.

of the droplets, the surface of the particles remains mostly smooth.

Emulsion droplet size and microspheres' dimensions are reported in Table 1 and their variations studied as a function of the respective flow rates of the chitosan solution and oil/surfactant mixture.

In the conditions investigated here, the microsphere diameter roughly ranges between 50 and $150 \mu\text{m}$ depending on the microfluidic chip geometry and respective phases flow rate. The overall trend is that for a fixed oil flow rate ("Qc"), increasing the chitosan flow rate ("Qd") results in increased particle size (Figure 3a). Similarly, increasing the oil flow rate at fixed chitosan flow rate produces smaller droplets. Therefore, the ratio Q_c/Q_d is the relevant parameter, in agreement with previous works [32–35].

Hybrid chitosan-collagen microspheres were prepared following the same procedure but with a mixed solution of collagen and chitosan (9:1) as the aqueous phase for the emulsion. The addition of a small proportion of collagen to the chitosan solution was intended to promote cell adhesion while keeping the viscosity relatively low. In fact, preliminary unpublished results suggested that cells (mesenchymal stem cells and PC12) did not readily adhere to pure chitosan microspheres. The dimensions of microspheres are also dependent upon the respective flow rates of the aqueous and oil phases (Figure 4). This effect is even stronger compared to pure chitosan solutions.

To assess the homogeneity of the mixtures at acidic pH, their turbidity was evaluated by measuring the intensity of light scattered at 90° as a function of the total polymer concentration for a fixed chitosan:collagen ratio of 9:1. Scattered light intensity increases linearly with increasing polymer

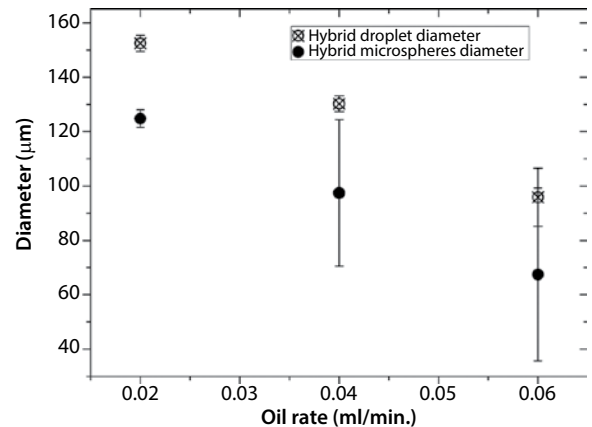


Figure 4 Size of hybrid chitosan-collagen emulsion droplets (crossed open circle) and microspheres after ammonia vapors (solid circles) as a function of oil flow rate at constant chitosan solution flow rate ($0.002 \text{ ml}\cdot\text{min}^{-1}$). Chip $100 \times 100 \mu\text{m}^2$ cross design.

concentration, suggesting that the mixed solutions remain homogeneous. Indeed, the formation of large aggregate would drastically increase the scattered light intensity, which is not observed here, notably at the concentration (2.1 wt%) used to prepare the hybrid microspheres. In fact, at this concentration, the scattered light intensity for the hybrid solution (3032 ± 54) was only slightly larger than the sum of intensities scattered by the corresponding individual solutions of 1.9 wt% chitosan (2102 ± 123) and 0.22 wt% collagen (518 ± 230). It should be noted that the pH of the mixture increased from approx. 3 to 4 over the entire concentration range (0.25–3 wt%). In this pH range, the net charge of both polymers, chitosan and collagen, remains mostly unchanged and

no particular change in behavior is thus expected. However, this does not rule out the possibility of local association between the charged amino groups of chitosan and partly charged acidic side chains from collagen (aspartatic or glutamic acid), resulting in a slight increase in scattered light. The repartition of the two polymers after solidification of the droplets was assessed by confocal microscopy observations of hybrid microspheres with a dual fluorescence labeling of chitosan (green, FITC) and collagen (red, TRITC) with chitosan-FITC:collagen-TRITC ratio of 9:1. The separate channels and overlay clearly indicate a homogenous co-localization of chitosan and collagen at the micrometer level (Figure 5b).

3.2 Cell Adhesion

Because the materials (chitosan and hybrid chitosan-collagen) are intended to support the differentiation of neural cells, we investigated the adhesion and survival of model PC12 cells on the microspheres. It should be noted that in the absence of microspheres, the cell culture plates being treated to prevent adhesion, the cells tend to form aggregates that remain in suspension. In the presence of microspheres, part of the cells adheres to the biopolymers surface. Cells in excess either remain in the medium and aggregate into dense clusters or form bridges between the microspheres (Figure 6). The adhesion rate is clearly

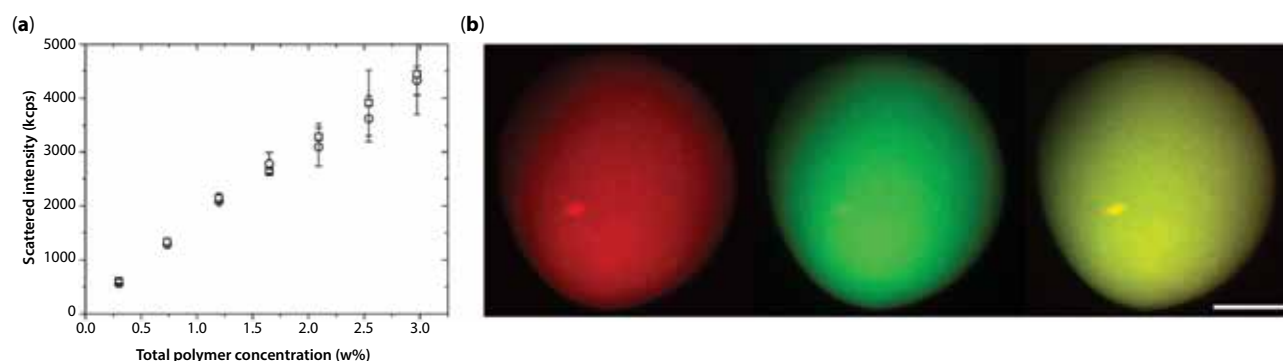


Figure 5 (a) Homogeneity of chitosan-FITC:collagen-TRITC solutions assessed by light scattering measurements as a function of total polymer concentration in wt%. (b) Maximum intensity projection of a Z-stack of 41 successive slices of a hybrid microsphere imaged by confocal microscopy, with collagen labeled in red (left), chitosan in green (center) and overlay (right). The bar is 50 μm .

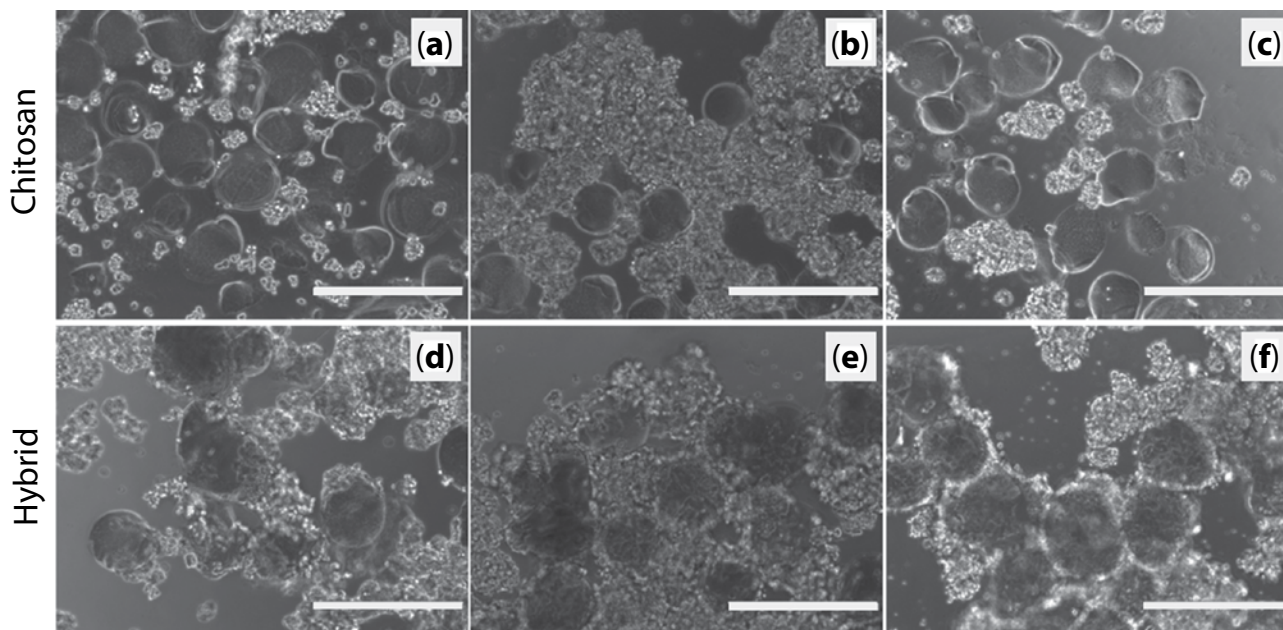


Figure 6 Optical micrographs of PC12 cells in the presence of microspheres made of either pure chitosan (a–c) or chitosan-collagen mixtures (d–f) after 24 h (a, d), 48 h (b, e) and 74 h (c, f) of incubation.

higher with hybrid particles (containing collagen) compared to pure chitosan ones, which is quantitatively confirmed in Figure 7. Chitosan has been largely described as a suitable biopolymer to elaborate implantable scaffolds for tissue regeneration [16, 36–38]. However, several previous studies have pointed out a rather low cell adhesion rate on the surface of chitosan hydrogel [39], which was compensated, for instance, by grafting adhesion peptides [40, 41] or addition of ECM molecules like collagen [42] or gelatin [39]. Additionally, a CyQUANT cell-counting assay revealed that cell survival is promoted by the presence of microspheres, the cell count after 24 hours in low adhesion culture plates being $6.59 \pm 1.17 \times 10^4$ cells in the absence of microspheres, $8.53 \pm 1.40 \times 10^4$ with chitosan microspheres ($\times 1.3$) and $9.85 \pm 1.28 \times 10^4$ in the presence of hybrid microspheres ($\times 1.5$). Since the CyQUANT assay is based on total DNA content, the total cell count is a combination of cell survival and proliferation. The reported doubling time for PC12 being approximately 92 hours [43], proliferation cannot account for the differences in cell count after 24 hours. Globally, in agreement with previous studies, our data indicate higher adhesion and survival rate in the presence of collagen combined with the chitosan microspheres.

3.3 Assembly and Gradient Formation

The present study was aimed at demonstrating the possibility of generating materials exhibiting protein functionalization gradients by assembling hydrogel microspheres. Such materials are intended to guide cells, in particular neural cells, by imposing a

chemo-attractive effect inducing migration and/or differentiation along a preferred direction. More precisely, the final objective was to elaborate tubular nerve guides. For practical reasons, we chose to first elaborate flat membranes that can be later rolled into tubular structures [36]. The membranes were obtained by the sedimentation of microspheres in a vertical flat mold and retrieved after crosslinking. To form gradients, we explored two routes: 1) mix gradually increasing proportions of functionalized microspheres with bare ones or 2) assemble successive layers of microspheres exhibiting an increasing level of functionalization (Figure 8a,b). We first optimized the assembly process with fluorescein-labeled microspheres (Figure 8a,b). Labeling with fluorescein was obtained by reacting the isothiocyanate moiety of FITC with the free amino groups of the biopolymers. The final objective being to functionalize the materials with active proteins such as growth factors, and in particular neurotrophins, using the same chemical approach. In the first instance, BSA was studied as a model protein to assess the efficiency of the coupling procedure. In this case, EDC was used to activate a diacid linker such as succinic acid. To graft the active protein onto the microspheres, one carboxylic group of the diacid should react with a free amino group of BSA and the second carboxyl group with a free amino group from chitosan or collagen. Microspheres were prepared by this procedure with increasing functionalization levels and assembled into membranes (Figure 8c). The profile of fluorescence intensity measured along the microspheres deposition direction clearly exhibits a linear fluorescence gradient (Figure 8d). The fluorescence profile is clearly distinct from the profile of transmitted light intensity, which

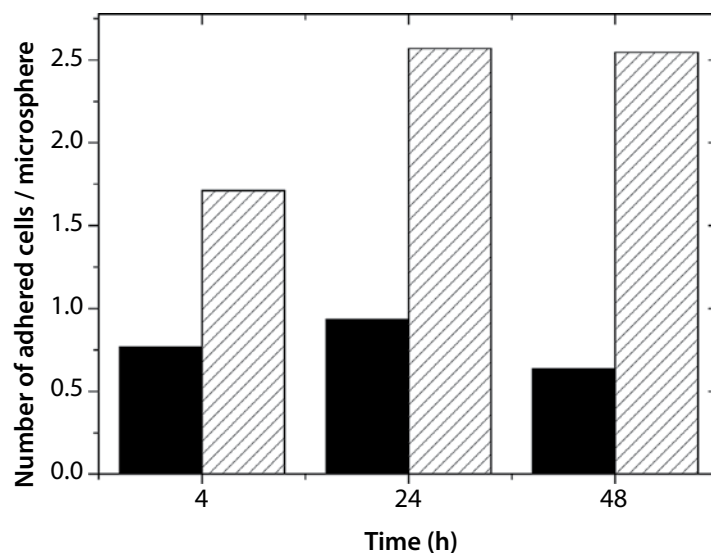


Figure 7 Comparison of the number of PC12 cells adhered onto chitosan (solid bars) and chitosan-collagen hybrid (hatched bars) microspheres after 4, 24 and 48 hours of culture.

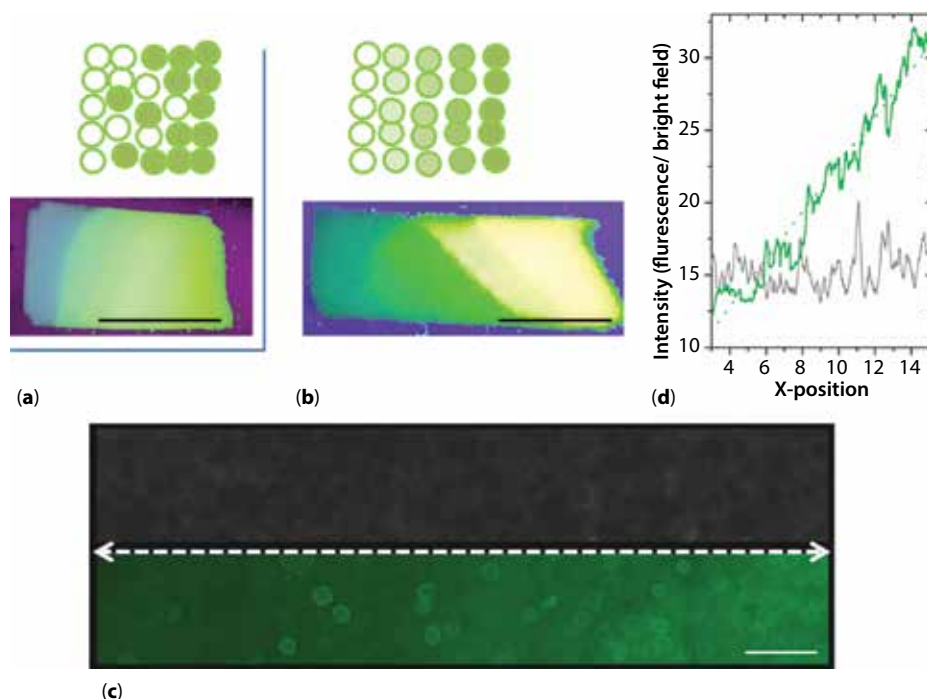


Figure 8 Formation of membranes with functionalization gradients either by mixing functionalized with non-functionalized particles (a), or by varying the functionalization level (b–d). (a, b) Macroscopic images of the FITC-functionalized materials under UV illumination; (c) microscopic observations of a membrane from microspheres functionalized with increasing BSA-FITC levels (left to right) observed in transmitted light (upper panel) or fluorescence (lower panel, green) and corresponding fluorescence intensity profile (d, x-position unit is $10^2 \mu\text{m}$) measured along the dashed white line in (c). Scale bars: a, b = 1 cm; c = $400 \mu\text{m}$.

appears noisy only because of variations in opacity at the micron scale due to the microspheres assembling.

4 CONCLUSIONS

Here we intended to demonstrate the possibility of elaborating materials exhibiting functionalization gradients by the assembly of microspheres of well-defined and adaptable dimensions. Contrary to bulk emulsion-based processes, the microspheres produced by micro- or milli-fluidic technologies show relatively narrow size distributions. In addition, the microsphere size could be varied by a factor of two by simply changing the flow rates of the solutions forming the emulsion. The solidification process, based on the precipitation of chitosan (with or without collagen added) by raising the pH of the droplets by the diffusion of ammonia vapors, leaves amine functions available for further functionalization of the particles and assembly. Hybrid microspheres exhibit a uniform repartition of chitosan and collagen, owing to the homogeneity of the initial acidic mixed solutions. The presence of small collagen amounts does not strongly impact the microfluidic processing of the solutions, but largely improves cell adhesion. The resulting microspheres, labeled with a

fluorescent dye or conjugated to a protein, were successfully assembled into materials exhibiting functionalization gradients. This proof-of-concept study can be extended to the generation of materials exhibiting growth factor gradients suited for the elaboration of tubular structures intended to guide neural growth.

ACKNOWLEDGMENTS

The authors thank L. Vachoud (rheology) and P. Gonzalez (HPLC) For their help with chitosan characterization. AD acknowledges the EPHE for providing a PhD fellowship.

REFERENCES

1. M.P. Lutolf, P.M. Gilbert, and H.M. Blau, Designing materials to direct stem-cell fate. *Nature* **462**, 433–441 (2009).
2. D. Seliktar, Designing cell-compatible hydrogels for biomedical applications. *Science* **336**, 1124–1128 (2012).
3. M. Ventre, F. Causa, and P.A. Netti, Determinants of cell–material crosstalk at the interface: Towards engineering of cell instructive materials. *J. R. Soc. Interface* **9**, 2017–2032 (2012).

4. X. Yao, R. Peng, and J. Ding, Cell-material interactions revealed via material techniques of surface patterning. *Adv. Mater.* **25**, 5257–5286 (2013).
5. S.L. Bechara, A. Judson, and K.C. Papat, Template synthesized poly(ϵ -caprolactone) nanowire surfaces for neural tissue engineering. *Biomaterials* **31**, 3492–3501 (2010).
6. B. Delalat, A. Mierczynska, S.R. Ghaemi, A. Cavallaro, F.J. Harding, K. Vasilev, and N.H. Voelcker, Materials Displaying Neural Growth Factor Gradients and Applications in Neural Differentiation of Embryoid Body Cells. *Adv. Funct. Mater.* **25**, 2737–2744 (2015).
7. N. Gomez, Y. Lu, S. Chen, and C. E. Schmidt, Immobilized nerve growth factor and microtopography have distinct effects on polarization versus axon elongation in hippocampal cells in culture. *Biomaterials* **28**, 271–284 (2007).
8. D.-H. Kim, H. Lee, Y.K. Lee, J.-M. Nam, and A. Levchenko, Biomimetic nanopatterns as enabling tools for analysis and control of live cells. *Adv. Mater.* **22**, 4551–4566 (2010).
9. C.K. Yeung, L. Lauer, A. Offenhäusser, and W. Knoll, Modulation of the growth and guidance of rat brain stem neurons using patterned extracellular matrix proteins. *Neurosci. Lett.* **301**, 147–150 (2001).
10. D. Santos, P. Wieringa, L. Moroni, X. Navarro, and J.D. Valle, PEOT/PBT guides enhance nerve regeneration in long gap defects. *Adv. Healthc. Mater.* **6**(3), 1600298 (2017).
11. X. Cao and M.S. Shoichet, Defining the concentration gradient of nerve growth factor for guided neurite outgrowth. *Neuroscience* **103**, 831–840 (2001).
12. M.R. Wrobel and H.G. Sundararaghavan, Directed migration in neural tissue engineering. *Tissue Eng. Part B Rev.* **20**, 93–105 (2013).
13. W. Zhu, C. O'Brien, J.R. O'Brien, and L.G. Zhang, 3D nano/microfabrication techniques and nanobiomaterials for neural tissue regeneration. *Nanomed.* **9**, 859–875 (2014).
14. S. García, R. Sunyer, A. Olivares, J. Noailly, J. Atencia, and X. Trepapat, Generation of stable orthogonal gradients of chemical concentration and substrate stiffness in a microfluidic device. *Lab. Chip* **15**, 2606–2614 (2015).
15. M. H. Struszczyk, Chitin and chitosan. Part I. Properties and production. *Polimery* **47**, 316–325 (2002).
16. I.-Y. Kim, S.-J. Seo, H.-S. Moon, M.-K. Yoo, I.-Y. Park, B.-C. Kim, and C.-S. Cho, Chitosan and its derivatives for tissue engineering applications. *Biotechnol. Adv.* **26**, 1–21 (2008).
17. F. Croisier and C. Jérôme, Chitosan-based biomaterials for tissue engineering. *Eur. Polym. J.* **49**, 780–792 (2013).
18. P. Sorlier, A. Denuzière, C. Viton, and A. Domard, Relation between the degree of acetylation and the electrostatic properties of chitin and chitosan. *Biomacromolecules* **2**, 765–772 (2001).
19. F. Gobeaux, G. Mosser, A. Anglo, P. Panine, P. Davidson, M.-M. Giraud-Guille, and E. Belamie, Fibrillogenesis in dense collagen solutions: A physicochemical study. *J. Mol. Biol.* **376**, 1509–1522 (2008).
20. S.-T. Lee, F.-L. Mi, Y.-J. Shen, and S.-S. Shyu, Equilibrium and kinetic studies of copper(II) ion uptake by chitosan-tripolyphosphate chelating resin. *Polymer* **42**, 1879–1892 (2001).
21. R. Parenteau-Bareil, R. Gauvin, and F. Berthod, Collagen-based biomaterials for tissue engineering applications. *Materials* **3**, 1863–1887 (2010).
22. H. Fujimaki, K. Uchida, G. Inoue, M. Miyagi, N. Nemoto, T. Saku, Y. Isobe, K. Inage, O. Matsushita, S. Yagishita, J. Sato, S. Takano, Y. Sakuma, S. Ohtori, K. Takahashi, and M. Takaso, Oriented collagen tubes combined with basic fibroblast growth factor promote peripheral nerve regeneration in a 15 mm sciatic nerve defect rat model. *J. Biomed. Mater. Res. A* **105**, 8–14 (2017).
23. S. Hong, H.-J. Hsu, R. Kaunas, and J. Kameoka, Collagen microsphere production on a chip. *Lab Chip* **12**, 3277–3280 (2012).
24. F. Gobeaux, E. Belamie, G. Mosser, P. Davidson, and S. Asnacios, Power law rheology and strain-induced yielding in acidic solutions of type I-collagen. *Soft Matter* **6**, 3769–3777 (2010).
25. Z. Chen, X. Mo, and F. Qing, Electrospinning of collagen-chitosan complex. *Mater. Lett.* **61**, 3490–3494 (2007).
26. L. Wang and J.P. Stegemann, Thermogelling chitosan and collagen composite hydrogels initiated with beta-glycerophosphate for bone tissue engineering. *Biomaterials* **31**, 3976–3985 (2010).
27. E. Rondeau and J.J. Cooper-White, Biopolymer micro-particle and nanoparticle formation within a microfluidic device. *Langmuir* **24**, 6937–6945 (2008).
28. M. Lavertu, Z. Xia, A.N. Serreji, M. Berrada, A. Rodrigues, D. Wang, M.D. Buschmann, and A. Gupta, A validated ¹H NMR method for the determination of the degree of deacetylation of chitosan. *J. Pharm. Biomed. Anal.* **32**, 1149–1158 (2003).
29. I. Bergman and R. Loxley, Two Improved and Simplified Methods for the Spectrophotometric Determination of Hydroxyproline. *Anal. Chem.* **35**, 1961–1965 (1963).
30. M. Mathieu, S. Vigier, M.N. Labour, C. Jorgensen, E. Belamie, and D. Noël, Induction of mesenchymal stem cell differentiation and cartilage formation by cross-linker-free collagen microspheres. *Eur. Cell. Mater.* **28**, 82–97 (2014).
31. A. Chenite, C. Chaput, D. Wang, C. Combes, M.D. Buschmann, C.D. Hoemann, J.C. Leroux, B.L. Atkinson, F. Binette, and A. Selmani, Novel injectable neutral solutions of chitosan form biodegradable gels in situ. *Biomaterials* **21**, 2155–2161 (2000).
32. S.L. Anna, N. Bontoux, and H.A. Stone, Formation of dispersions using “flow focusing” in microchannels. *Appl. Phys. Lett.* **82**, 364–366 (2003).
33. H. Zhang, E. Tumarkin, R. Peerani, Z. Nie, R.M.A. Sullan, G.C. Walker, and E. Kumacheva, Microfluidic production of biopolymer microcapsules with controlled morphology. *J. Am. Chem. Soc.* **128**, 12205–12210 (2006).
34. T. Nisisako, T. Torii, and T. Higuchi, Novel microreactors for functional polymer beads. *Chem. Eng. J.* **101**, 23–29 (2004).

35. J.D. Wehking, M. Gabany, L. Chew, and R. Kumar, Effects of viscosity, interfacial tension, and flow geometry on droplet formation in a microfluidic T-junction. *Microfluid. Nanofluidics* **16**, 441–453 (2014).
36. V. Chiono and C. Tonda-Turo, Trends in the design of nerve guidance channels in peripheral nerve tissue engineering. *Prog. Neurobiol.* **131**, 87–104 (2015).
37. W. Daly, L. Yao, D. Zeugolis, A. Windebank, and A. Pandit, A biomaterials approach to peripheral nerve regeneration: Bridging the peripheral nerve gap and enhancing functional recovery. *J. R. Soc. Interface* **9**, 202–221 (2012).
38. A.R. Nectow, K.G. Marra, and D.L. Kaplan, Biomaterials for the development of peripheral nerve guidance conduits. *Tissue Eng. Part B Rev.* **18**, 40–50 (2012).
39. W. Xia, W. Liu, L. Cui, Y. Liu, W. Zhong, D. Liu, J. Wu, K. Chua, and Y. Cao, Tissue engineering of cartilage with the use of chitosan-gelatin complex scaffolds. *J. Biomed. Mater. Res. B Appl. Biomater.* **71B**, 373–380 (2004).
40. X. Liu, W. Peng, Y. Wang, M. Zhu, T. Sun, Q. Peng, Y. Zeng, B. Feng, X. Lu, J. Weng, and J. Wang, Synthesis of an RGD-grafted oxidized sodium alginate–N-succinyl chitosan hydrogel and an in vitro study of endothelial and osteogenic differentiation. *J. Mater. Chem. B* **1**, 4484–4492 (2013).
41. L.M.Y. Yu, K. Kazazian, and M.S. Shoichet, Peptide surface modification of methacrylamide chitosan for neural tissue engineering applications. *J. Biomed. Mater. Res. A* **82A**, 243–255 (2007).
42. B. Choi, S. Kim, B. Lin, B.M. Wu, and M. Lee, Cartilaginous extracellular matrix-modified chitosan hydrogels for cartilage tissue engineering. *ACS Appl. Mater. Interfaces* **6**, 20110–20121 (2014).
43. L.A. Greene and A.S. Tischler, Establishment of a noradrenergic clonal line of rat adrenal pheochromocytoma cells which respond to nerve growth factor. *Proc. Natl. Acad. Sci. U. S. A.* **73**, 2424–2428 (1976).